REPORT

Effect of riverbed sediment flushing and clogging on river-water infiltration rate: a case study in the Second Songhua River, Northeast China

Geng Cui[1,2] · Xiaosi Su[2] · Yan Liu[3] · Shida Zheng[2]

Abstract
Infiltration from natural rivers or streams is the most important source of aquifer recharge at riverbank filtration (RBF) sites. Due to the influence of river hydrological processes and changes in suspended solids in rivers, riverbed sediments often undergo significant flushing and clogging processes, which lead to obvious spatial and temporal changes in riverbed sediment permeability. Moreover, the lithology, structure, and thickness of natural riverbed sediments change with time, influencing the bank infiltration rate into groundwater. At present, how riverbed-sediment flushing and clogging influences the sediment hydraulic conductivity is not fully understood, which results in high uncertainty about the amount of water involved in RBF. An RBF site in the middle reach of the Second Songhua River, northeastern China, was studied, and continuous time series data of riverbed-sediment hydraulic conductivity were obtained for the first time. By identifying the hydrological conditions, using field monitoring, laboratory experiments and field tests, the mechanisms of change associated with sediment lithology, infiltration rate, and hydraulic conductivity during flushing and clogging processes were revealed.

Introduction

Pumping groundwater from the banks of perennial rivers (riverbank filtration, RBF) is a highly efficient way to increase groundwater resources, by inducing the recharge of groundwater via river water. Owing to the advantages of easy groundwater extraction and management, effective purification of surface water, and stability of water supply, RBF has become an important way to develop and utilize water resources (Ahmed and Marhaba 2016; Farnsworth and Hering

✉ Xiaosi Su
  suxiaosi@163.com

1   Northeast Institute of Geography and Agroecology, Chinese Academy of Sciences, Changchun 130102, China

2   Institute of Water Resources and Environment, Jilin University, Changchun 130021, China

3   College of New Energy and Environment, Jilin University, Changchun 130021, China

2011)—for example, RBF along the rivers Rhine and Elbe in Germany has been operated for hundreds of years (Schubert 2003; Fischer et al. 2005; Ray et al. 2002). In addition, the proportion of RBF water accounts for 50 and 45% of drinking water in Slovakia and Hungary, respectively (Farnsworth and Hering 2011; Bourg and Bertin 1993). Additionally, RBF is also a common groundwater resource management strategy in Northern China; for example, it is performed at filtration sites along the Yellow River at Jiuwu Beach in the city of Zhengzhou (Liao et al. 2004), the Songhua River in the city of Jiamusi (Wang et al. 2006), and the Liao River in the city of Shenyang (Su et al. 2017a; Su et al. 2018).

Revealing the river infiltration rate is crucial when evaluating the groundwater resources of the RBF site, and the permeability of riverbed sediments is a key parameter determining the amount of river-water infiltration (Crosbie et al. 2014; Harvey and Gooseff 2015). Riverbed sediments are the key layer for river-water infiltration and groundwater recharge, which can not only affect the amount of infiltration (Jolly et al. 2008; Frei et al. 2009; Anibas et al. 2011), but also change the retention time of filtrated river water, nutrient flux, and groundwater acid-base and redox conditions, further affecting the biogeochemical reactions in riverbed sediments

and the extent of removal of pollutants from the river water during RBF (Su et al. 2017b).

As well as the hydraulic gradient between the river stage and water table, the infiltration rate of river water is significantly affected by the permeability of riverbed sediments, which depends mainly on the sediment lithology, structure, and thickness. Generally, studies have shown that along the flow direction, the river flow velocity continuously decreases, kinetic energy is continuously lost, and transported particles vary in type and size from the source of the river to the estuary (Gurnell et al. 2012; Nosrati 2017; Mueller and Pitlick 2013). Therefore, the changes along a river in terms of regulation, flow path, erosion and sedimentation also affect the composition, structure, and thickness of the riverbed sediment, resulting in strong spatial variability in the riverbed sediment's permeability. The flushing and clogging processes of riverbed sediments in different seasons, associated with incoming and outgoing sand movement, will cause the permeability of the riverbed to vary with time (Leonardson 2011; Stewardson et al. 2016; Grischek and Bartak 2016). This spatial and temporal variability in riverbed sediment permeability, which is often up to 1–2 orders of magnitude, directly affects the temporal and spatial variation in the bank infiltration rate. Existing studies mainly focus on the influence of riverbed clogging, which has been defined as the process of permeability reduction. Riverbed clogging is caused by: the infiltration or deposition of sediment particles, organic solids and inorganic solids in surface water; the precipitation of carbonate, iron, and manganese hydroxides or oxides; and a series of biological processes that lead to the formation of a silt layer on the surface of the riverbed (Datry et al. 2015; Grischek and Bartak 2016; Zhang et al. 2011; Blaschke et al. 2010; Nogaro et al. 2010). Clogging is classified into four types: physical clogging (precipitation, infiltration of suspended solid particles), mechanical clogging (gas entrapment), biological clogging (bacterial growth and reproduction; Battin and Sengschmitt 1999; Baveye et al. 1998), and chemical clogging (precipitation, complexation reaction) (Stéphanie et al. 2000). The type of clogging and the influencing factors have been explored through sediment sample collection and analysis, resistivity imaging, physical simulation experiments, and soil column experiments (Danczak et al. 2016; Febria et al. 2010; Goldschneider et al. 2007; Pholkern et al. 2015; Seifert and Engesgaard 2007; Engesgaard et al. 2006; Ulrich et al. 2015); however, it is rarely reported how the flushing process affects the permeability of riverbed sediments.

The hydraulic conductivity (K) of the riverbed sediment is closely associated with its permeability. From the 1990s, researchers began to pay attention to the spatial variability in riverbed-sediment hydraulic conductivity and proposed a variety of methods to measure it, including laboratory analysis, numerical modeling, tracing, and direct field measurement methods (Cey et al. 1998; Lee 1979; Springer et al. 1999;

Rosenberry 2000; Su et al. 2004; Hart et al. 1999). Among them, the heat-tracing method is environmentally friendly, simple, rapid, reliable, and economical, and it is easy to acquire related parameters (Su et al. 2016, 2002). Therefore, the heat-tracing method was selected for this study to calculate the infiltration rate of river water, and combined with the vertical pore-water head difference, the hydraulic conductivity of the riverbed sediments is calculated.

The Second Songhua River is a perennial river in northeastern China, whose basin covers a wide area. There are many groundwater abstraction sites along the Second Songhua River corridor, which are important water supply sources for industrial and domestic uses in the coastal areas. Due to the changes in river hydrodynamic conditions, there are obvious spatial variations in the composition, structure, and thickness of riverbed sediments from upstream to downstream areas. The Gaojiadian groundwater source site, adjacent to the Dacheng Dehui Industrial Park in Changchun, is a typical RBF site along the Second Songhua River. Since the current groundwater exploitation plan can no longer meet the industrial production needs, the scale of groundwater exploitation needs to be expanded. However, whether there is sufficient supply resource when increasing the extraction amount, and consequently changing the river infiltration rate, is still not understood. For this reason, this study has two objectives: (1) to analyze the influence of river hydrological conditions on the river-bed sediment lithology and bank infiltration rate and (2) to obtain time series data of riverbed-sediment hydraulic conductivity. Therefore, it is necessary and urgent to study the influence of sediment flushing and clogging on the river infiltration rate, since it can provide an important scientific basis for evaluating the groundwater resources at the RBF site and for rational planning of the groundwater extraction.

Materials and methods

Study area

The Gaojiadian groundwater source site is located on the east side of the village of Gaojiadian approximately 8 km northeast of the town of Caiyuanzi, Dehui City, Jilin Province (Fig. 1), at geographical coordinates 125°52′00″–125°54′20″E, 44°47′00″–44°48′40″N. Monitoring and sampling stations in the riverbed are shown in Fig. 1.

The stage and flow hydrograph obtained from the Songhua River Hydrological Station located in the Second Songhua River main stream from September 2012 to September 2017 is shown in Fig. 2. The target river of this study, which ranges from 240 to 700 m wide, is located 2.5 km downstream of the Songhua River Hydrological Station, and the average annual runoff is 156×10^8 m^3/year (Songhuajiang Hydrological Station). The river runoff in the study area varies greatly
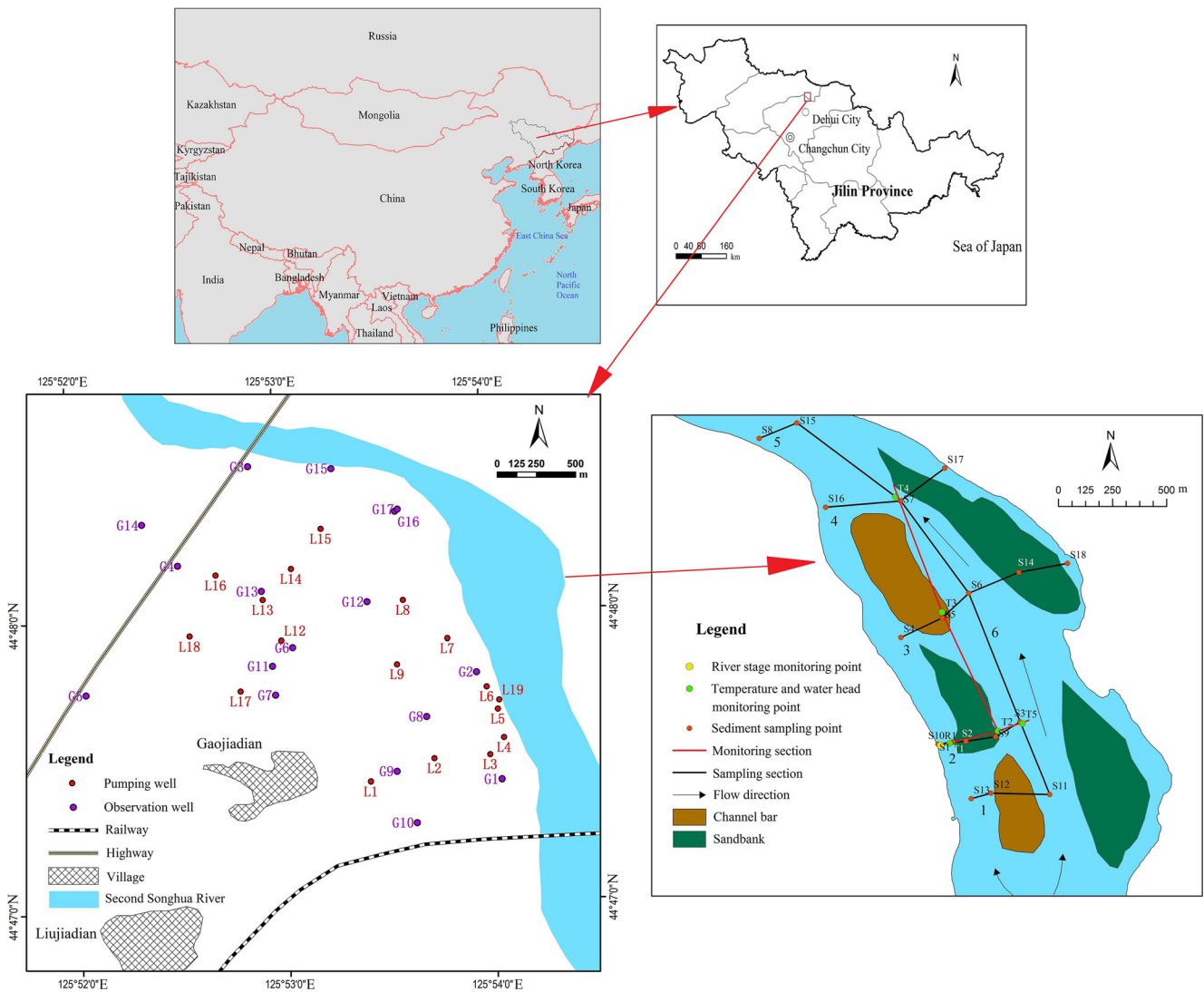
**Fig. 1** Location of the study area and monitoring and sampling stations

during the year through effects of precipitation, snowmelt runoff, and reservoir storage (Fengman Reservoir is 178 km upstream of the study area). Most flooding occurs in July, August, and September, which accounts for 60–70% of the total annual runoff. Spring floods often occur in May and June, and account for approximately 20% of the total annual runoff, while winter runoff is generally less than 5% of the total. Usually, at the end of March or the beginning of April every year, the snow and ice melt, and the river stage begins to rise, starting with a long spring flood. After the spring flood, due to only a small amount of precipitation in the late spring, the river stage is temporarily low. In the summer and autumn, the rainfall is concentrated, causing the summer and autumn floods. By the end of November, the river begins to freeze, and during the study period the ice thickness increased to about 0.9 m at the end of January in each year.

The riverbed sediments are mainly medium-fine sand. The main stream of the Second Songhua River mainly receives

water from precipitation and snow melt which forms surface runoff. The suspended solids content in the river water is low, and the sediment particles are mainly transported by traction or saltation. According to the measured data of Songhua River Hydrological Station from 2007 to 2010, the average suspended solids content is 0.051 kg/m^3 during the dry season and 0.115 kg/m^3 during the wet season.

The studied land area belongs to the river valley plain landform type, and the elevation range is 147.85–154.38 m above sea level (asl). The river valley of the study area alternates between the river floodplain and the meandering river valley. The upstream stretch is a wide and straight riverbed (shallow water zone), and the downstream is a narrow curved riverbed (deep water zone; Fig. 3). The water depth of the main channel is generally 2–8.5 m. In recent years, due to sand mining activities in the downstream portion of the study area, the water depth can reach 12 m; however, the sand quarry, which was located in the deep zone approximately 2,000 m from the

Fig. 2 Stage and flow hydrograph from September 2012 to September 2017 at the Songhua River Hydrological Station
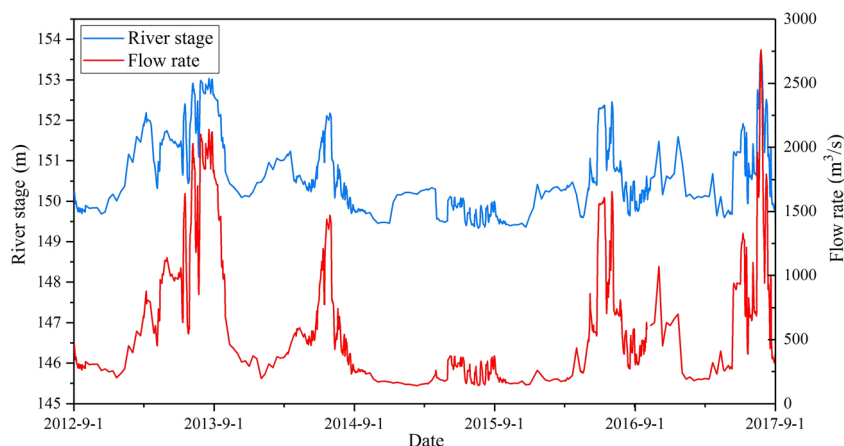
starting point downstream, was closed in 2016. The riverbed landforms are mainly erosional landforms (deep troughs) and accumulation landforms (beach, channel bars, and sandbanks; Fig. 1).

Water level and temperature monitoring

Five monitoring points (T1–T5) were installed to continuously monitor the water temperature and pore-water heads of riverbed sediments at different depths under different hydrological conditions during several water-inflow and runoff-recession events from May 16th to Aug. 14th, 2018, allowing estimation of the hydraulic conductivity of riverbed sediments (Fig. 4). Point T1 is located at the edge of the sandbar, T2 is located at the junction of the main channel and the sandbank, T3 and T4 are located at the upper and lower reaches of the channel bar respectively, and T5 is located in the main channel of the river. Three self-recording temperature loggers (TidbiTv2, UTBI-001 Onset Inc., USA) and two self-recording water level loggers (U20–001-04 Onset Inc., USA) were placed at each monitoring point. The cross-sectional schematic diagram of the monitoring points is shown in Fig. 4. Temperatures were recorded every 15 min at depths of 0, 20, and 80 cm below the riverbed surface at a precision of 0.02 °C. Pore-water heads were recorded every 15 min at 20 and 80 cm below the

riverbed surface, and the river stage was recorded at the same frequency at point R1.

Heat tracing

The infiltration rate of the river was calculated by the one-dimensional (1D) steady-flow heat transport model established by Stallman (1965), as follows:

$$\frac{\lambda_e}{\rho c}\frac{\partial^2 T}{\partial z^2} - q\frac{\rho_w c_w}{\rho c}\frac{\partial T}{\partial z} = \frac{\partial T}{\partial t} \tag{1}$$

where T is the temperature (°C), t is the time (day), z is the thickness of the sediments (m), q is the water flow rate (m³/day), ρ_w is the density of water (kg/m³), and λ_e is the effective thermal conductivity of the saturated sediment (Stallman 1965). Physical parameters such as thermal conductivity and specific heat of water and solid media were measured using a BRR specific heat capacity tester on the riverbed sediments and sediment pore-water samples at the study site.

The calculation of infiltration rate of the river water was realized by the MATLAB-based VFLUX module developed by Gordon et al. (2012). For a given set of temperature-time series from a single vertical sensor profile at a specific depth, the VFLUX program will (1) format and synchronize all the

Fig. 3 Bed bottom elevation of the longitudinal section
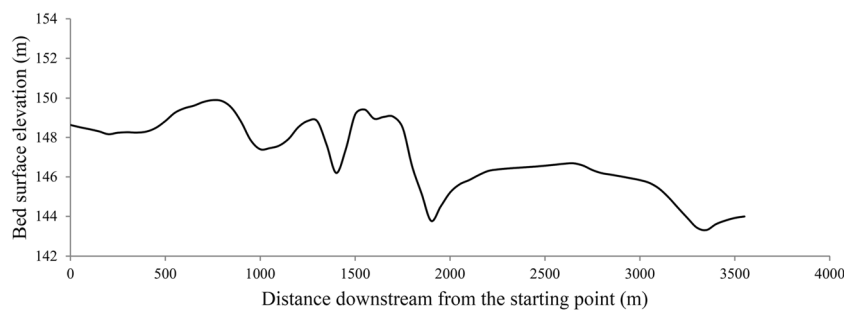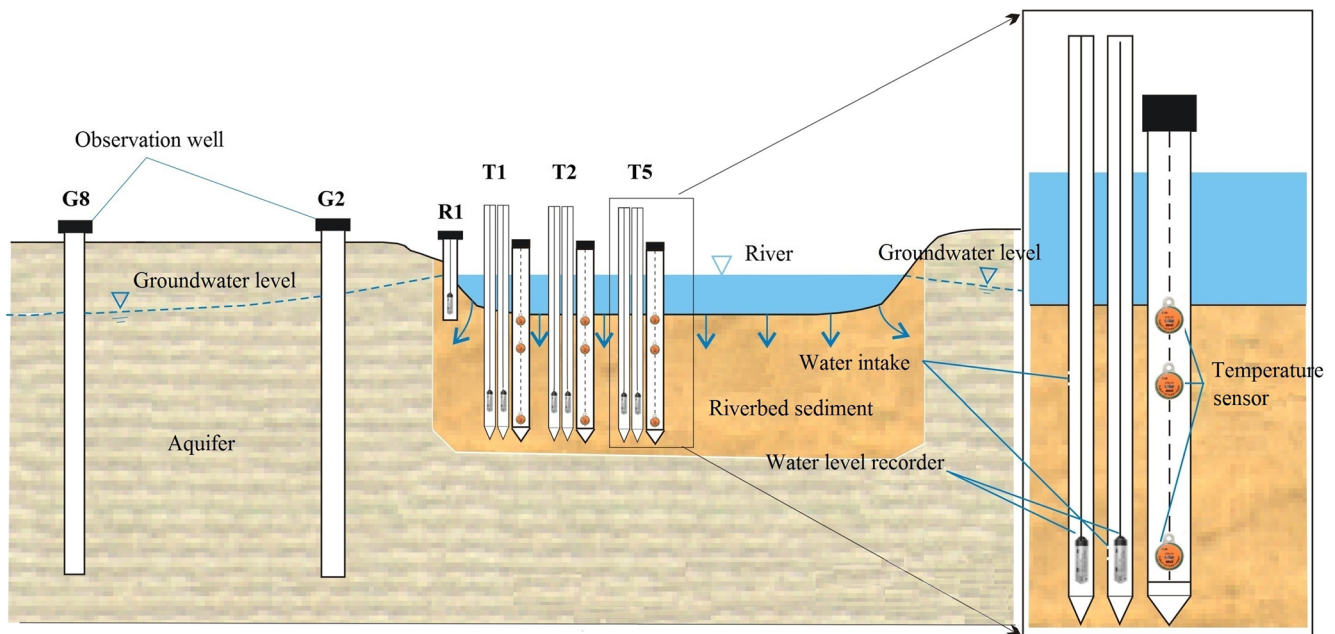
Fig. 4 Schematic diagram of the monitoring-point cross section

time series to a single vector of sampling times, (2) run a low-pass filter and resample the time series, (3) isolate the fundamental signal (the signal of interest, typically diurnal) using dynamic harmonic regression (DHR), (4) extract amplitude and phase information for the fundamental signal using DHR, (5) identify pairs of sensors based on one or more sliding analysis windows, and (6) calculate vertical water flux rates between the identified sensor pairs (Gordon et al. 2012).

Riverbed sediment sampling

Riverbed sediments were collected during the dry season (May 20th), the water inflow period of the first flood process (July 20th) and the runoff recession period of the second flood process (October 30th; Fig. 5). The sediment was collected using a Beeker sampler in the river by boat.

Markers were inserted in the sediments at the collection point so that the positions of multiple collection campaigns were exactly the same. The sampling depth was 0–50 cm below the riverbed surface, at intervals of 0–10, 10–30, and 30–50 cm below the riverbed surface. After the sample was collected, it was quickly placed in a PVC tube for particle size analysis in the laboratory using the sieving method and a laser particle size analyzer (Bettersize2000) to obtain the sediment lithology change information during flooding.

Empirical formula calculation

Odong (2007) compared a variety of empirical formulas for determining the hydraulic conductivity of particles ranging in size from gravel to fine sand. The Kozeny-Carman equation is one of the most widely accepted and most commonly

Fig. 5 River stage hydrograph of the study area and periods of the bed-sediment sample collection campaign (blue column)
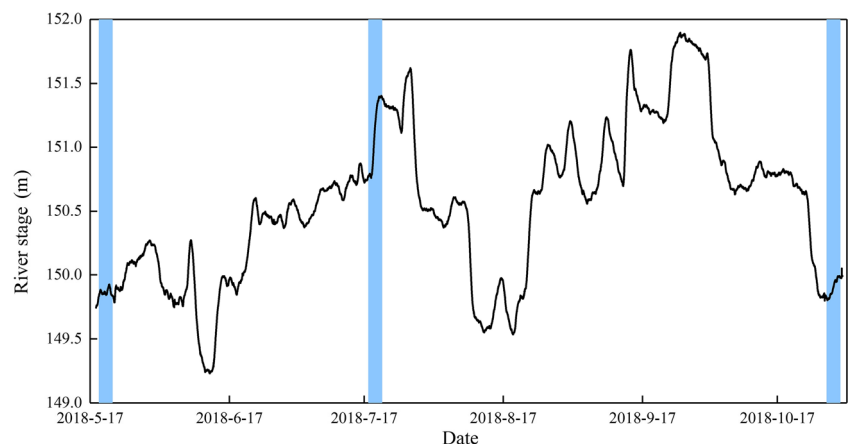
employed derivations of hydraulic conductivity as a function of the characteristics of the soil medium. This equation was originally proposed by Kozeny (1927) and was then modified by Carman (Carrier 2003) to become the Kozeny-Carman equation. For gravel sand, compared with the Breyer and Hazen formula, the Kozeny-Carmen formula more accurately estimates sediment hydraulic conductivity in this study. Therefore, the Kozeny-Carmen formula was used to estimate the riverbed sediment hydraulic conductivity in this study. The formula is as follows:

$$K = \frac{g}{v} \times 8.3 \times 10^{-3} \times \left(n^3/(1-n)^2 \right) \times d_{10}^2 \qquad (2)$$

where K is the hydraulic conductivity, g is the gravitational acceleration, v is the kinematic viscosity, n is the porosity, and d_{10} is the grain diameter (mm) by which 10% of the sample has grains of finer diameter than this value. The results were also compared to that calculated based on the following standpipe experiment method.

Standpipe experiment

The standpipe experiment was used to directly measure the sediment hydraulic conductivity of different thicknesses below the sediment surface. Relevant experimental data were recorded and the sediment hydraulic conductivity in the range of 0–10, 0–30, and 0–50 cm below the surface of the riverbed was calculated according to the formula by Hvorslev (1951):

$$K_v = \frac{\frac{\pi D}{11m} + L_v}{(t_2 - t_1)} \ln(h_1/h_2) \qquad (3)$$

$$K_{v2} = L_2 / \left(\frac{L}{K_v} - \frac{L_1}{K_{v1}} \right) \qquad (4)$$

where L_v is the thickness of the sediment in the vertical pipe, h_1 and h_2 are the water levels in the pipe at time t_1 and t_2, respectively, and D is the diameter of the pipe. According to Chen's (2004) findings, $m = 1$ represents isotropic deposits and $m = 10$ represents anisotropic deposits. In this calculation, m is defined as 10.

Results

Hydrodynamic conditions

The main driving factor of riverbed flushing and clogging is the temporal and spatial variation in hydrodynamic conditions (Gorman et al. 2007; Simpson and Meixner 2010).

Hydrodynamic conditions mainly include flow velocity, flow flux, and river stage. It can be seen from the stage-velocity-flux diagram (2007–2010) of the Songhua River Hydrological Station based on historical data (Fig. 6) that there is a significant positive correlation among flow rate, flow flux, and river stage. Combined with the riverbed elevation changes in Fig.7, riverbed sediment clogging occurred continuously from 2007 to 2010 at the riverbed 220 m from the west bank, and the flushing effect dominated from 2007 to 2010 at the riverbed 400m from the west bank. The significant differences in clogging and flushing process at different locations of the riverbed indicate that the flow velocity, flow flux, and river stage differ drastically along the hydrological monitoring section.

During the monitoring period of this study (from May 17th to Nov. 1st, 2018), the river stage of the Second Songhua River showed obvious changes affected by the seasons, precipitation, and the regulation of the upstream Fengman Reservoir. The river stage data at the monitoring point in the study area are shown in Fig. 6. It can be seen that from May 2018 to November 2018, the river experienced two distinct flood events (from June 16th to August 15th, and from August 22nd to October 30th), whereby the river stage variation reached 2.4 and 2.2 m, respectively.

Variation in sediment lithology during flushing and clogging processes

Temporal variation

It can be seen from the trend in Fig. 8 that the arithmetic average particle size at different depths of riverbed sediment changes with time from the main channel and from the edge of the sandbank, to the edge of the downstream channel bar.

At the edge of the sandbank (Fig. 8a), the particle size of sediment 0–10 cm deep varies greatly; it is 0.406 mm in the wet season and 0.269 mm in the dry season, varying by 0.137 mm. While the particle size range is smaller at 10–30 cm deep, the variation is 0.064 mm. The particle size is almost stable at 30–50 cm deep with a difference of 0.022 mm, which indicates that the hydrodynamic conditions (shear stress and shear flow rate) are weak at this location, and it is only affected by flushing and clogging of the surface sediments.

Compared with the main channel (Fig. 8d), the surface sediment particle size changed more clearly at the junction of the main channel and the edge of the sandbank (Fig. 8b), where the difference was 0.045 and 0.1 mm, respectively. At the same time, the particle size of sediment 30–50 cm deep in the main channel (Fig. 8d) was significantly larger in July than in the dry season from May to November, indicating that it is affected by river hydrodynamics. The thickness of sediment flushing and clogging in the riverbed could reach 50 cm in the

Fig. 6 Stage-velocity-flux diagram from Songhua River Hydrological Station
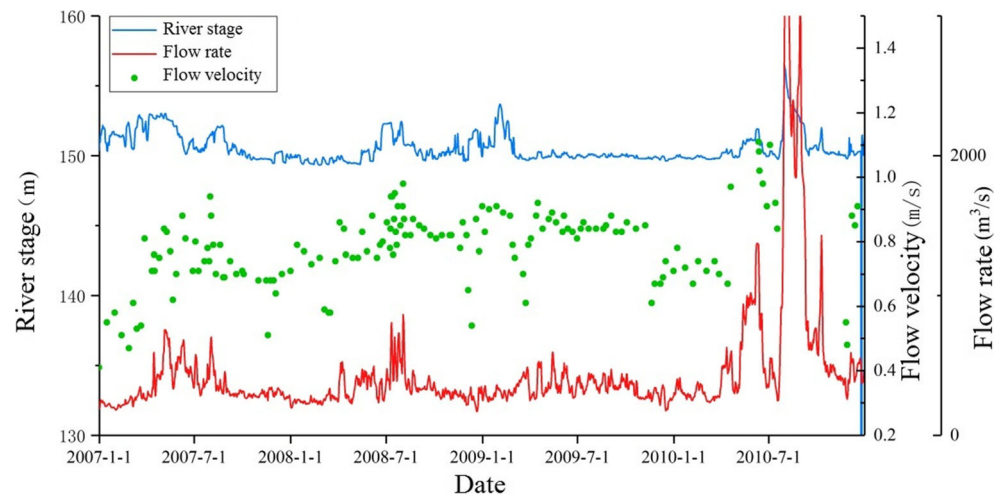
wet season, and the lithology of sediments 0–50 cm below the sediment surface was completely changed under the influence of flushing and clogging. At the edge of downstream channel bar (Fig. 8c), the grain size of the sediments at different depths showed an increasing trend with time, indicating that the channel bar moved downstream gradually.

Spatial variation

According to the results of the standpipe experiments, the relationship of the sediment hydraulic conductivity (K) and the arithmetic average particle size along the river longitudinal section (section 6 in Fig. 1) in November 2018 is shown in Fig. 9.

The K value of riverbed sediments ranges from 4.0 to 52.4 m/day from upstream to downstream, showing a fluctuation of first decreasing, then increasing, and decreasing again, which is consistent with the trend of the average particle size of the sediment, indicating that K is greatly affected by the sediment lithology. The K value is the

largest in the middle reaches (S6) at 52.4 m/day and decreases sharply in the middle and lower reaches (S7, S15). This is due to the weaker hydrodynamic force and slower flow rate caused by the influence of the flow resistance near the sandbank (S7), and deposition of fine particles in the river water leads to reduced hydraulic conductivity of the sediment. The main channel (S15) is narrowed and curved where the riverbed flushing is strong, resulting in a sudden drop in the riverbed elevation (slope increase), increased shear stress on the surface of the riverbed, and an increase in water depth; the deposition of fine sand or clay results in reduced hydraulic conductivity of the sediments (Fig. 9).

Using the third cross-section (section 3 in Fig. 1) as an example, the relationship between bed sediment hydraulic conductivity (K) and average particle size along the river cross-section in November 2018 is shown in Fig. 10. The trend of the K value is consistent with that of the average particle size. The K values of the deep groove of the west bank and the central main channel are larger, 31.0 m and

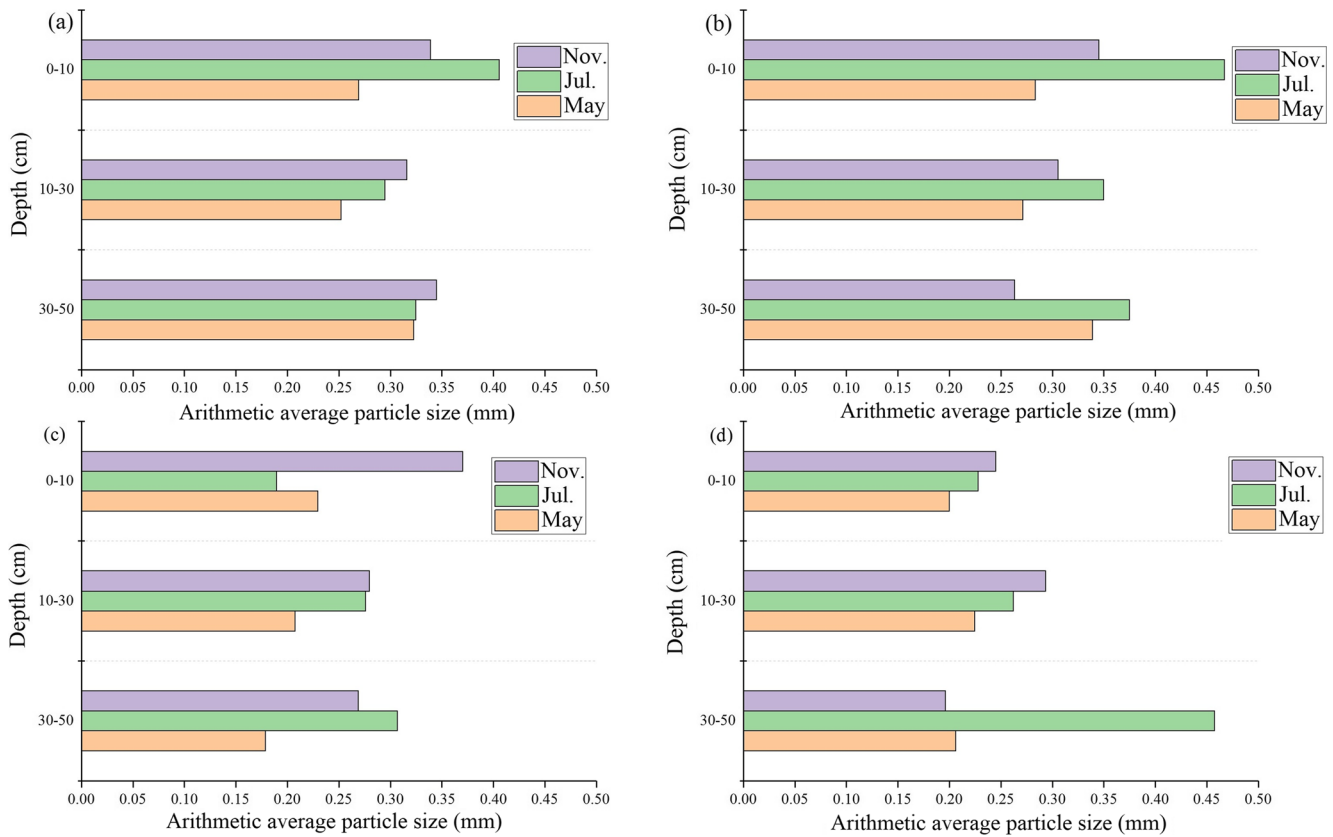**Fig. 7** Riverbed elevation changes from 2007 to 2010
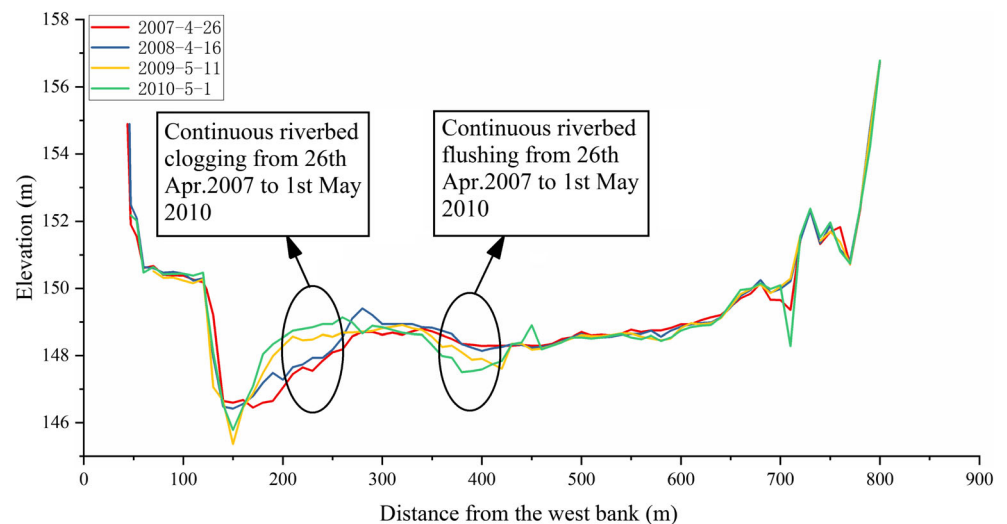
Fig. 8 Changes of arithmetical mean grain size of riverbed sediments at different depths and positions (**a** edge of sandbank, **b** junction of the main channel and the edge of sandbank, **c** channel bar and **d** main channel)

52.4 m/day, respectively, and significantly higher than the channel bar (4.1 m/day), sandbank (9.0 m/day), and the edge of the river bank (0.0016 m/day), showing that the effects of riverbed topography on sediment hydraulic conductivity are significant. The weak hydrodynamic conditions at the island, the sandbank, and the edge of the riverbank lead to the formation of finer-sediment particles and the deposition of a layer of silty clay, resulting in reduced K value. However, coarser particles deposit in the deep groove and the main channel under the influence

of stronger hydrodynamic conditions, resulting in larger K value of the sediments (Fig. 10).

Variation in bank infiltration rate during flushing and clogging processes

The test results of relevant parameters with the heat tracing method were as follows: the effective thermal conductivity was 1.88 W/m·K; the density and specific heat of the water were, respectively, 11,030 kg/m^3 and 4,063 J/kg·K, and of the sediment medium they were 1,400 kg/m^3 and 1,495 J/kg·K.

Fig. 9 Variation in sediment hydraulic conductivity along the river longitudinal section
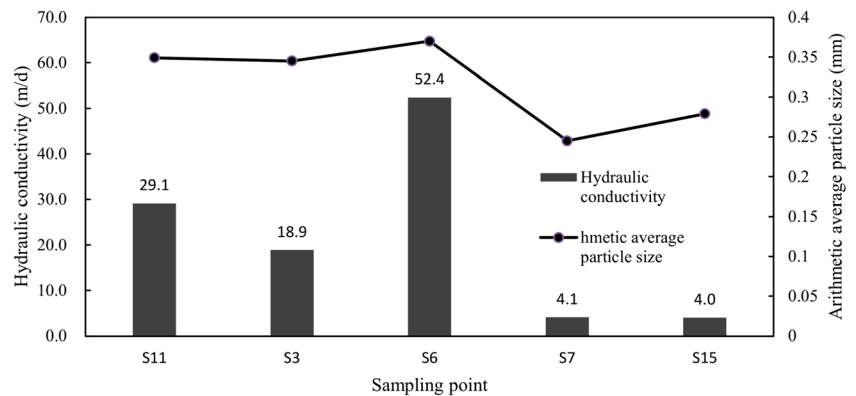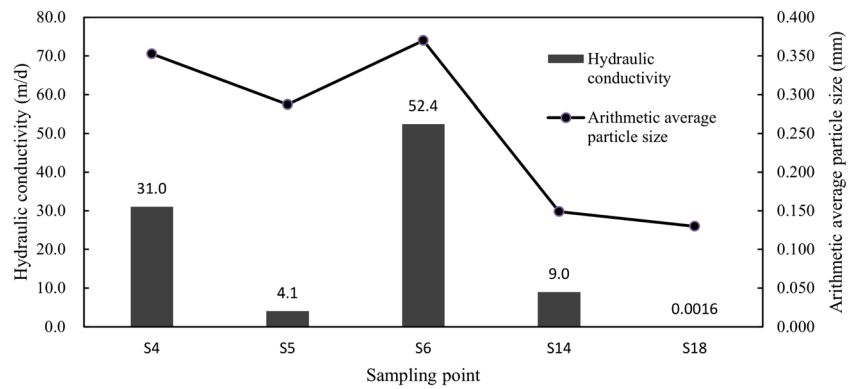
Fig. 10 Variation in sediment hydraulic conductivity along the river cross section

The characteristics of the spatial and temporal variation of the river-water infiltration rate (seepage velocity of shallow riverbed sediments) calculated by temperature signals at different riverbed sediment depths, and the dynamic change curve of the river-water level are shown in Fig. 11 (where May 16, 2018, was the starting point).

Using May 16, 2018, as the starting point, it can be seen from Fig. 11 that the maximum and minimum stage of the river are 151.618 and 149.229 m, respectively, with a difference of 2.389 m within 0–90 days. The range variation of river-water infiltration rate at the sandbank (T1, T2) was -1.2–3.0×10^{-6} m/s and 0.8–6.5×10^{-6} m/s, respectively, while it was -1.4–3.0×10^{-6} m/s and -0.7–4.0×10^{-6} m/s at the channel bar (T3, T4), and -1.1–6.0×10^{-6} m/s at the main channel (T5).

The variation trend of the river-water infiltration rate in the riverbed sediments has some correlation with the river stage fluctuation; that is, each fluctuation will cause an obvious change in infiltration rate. With a sudden increase in river stage, flow velocity and flux changes occur, the fine riverbed sediment particulates on the surface are washed downstream under the strong hydrodynamic action, and the coarser particles deposit simultaneously, resulting in a higher vertical hydraulic conductivity of the sediment. Under the drive of larger hydraulic gradient and sediment hydraulic conductivity, the river-water infiltration rate increased significantly. With a sudden drop of the river stage, flow velocity and flux changes occur, and the suspended load drops out of suspension to form silt layers of varying thickness that eventually form the bed sand, resulting in a decrease in vertical hydraulic conductivity of the sediment. When the hydraulic gradient is small and sediment hydraulic conductivity is low, the river-water infiltration rate decreases significantly. The water flow direction recorded by riverbed sediments will alternate from top to bottom and from bottom to top under the influence of changes in the hydrodynamic condition and the groundwater exploitation plan at the groundwater source site.

Variation in sediment hydraulic conductivity during flushing and clogging processes

Calculation and verification of riverbed sediment hydraulic conductivity

Based on Darcy's Law (Domenico and Schwartz 1997):

$$q = K \cdot J \tag{5}$$

where q represents the infiltration rate, K represents the riverbed sediment hydraulic conductivity, and J represents the hydraulic gradient within a certain depth of the sediment (Fig. 12). The hydraulic conductivity (K) of riverbed sediment (Fig. 13) at all monitoring points can be calculated from time series data of infiltration rates (q) (Fig. 11) and hydraulic gradient (J) obtained from the sediment pore-water head within the riverbed sediment. The fluctuation range of the sediments' hydraulic conductivity in each layer at each monitoring point is shown in Table 1. At some monitoring points such as T2, the temperature sensor was exposed to the river water due to strong flushing during flooding, which resulted in the distortion of temperature data and the absence of hydraulic conductivity data.

Sediment hydraulic conductivity was calculated by heat tracing, a standpipe experiment, and the Kozeny-Carmen empirical formula, and the results are compared in Fig. 14, which
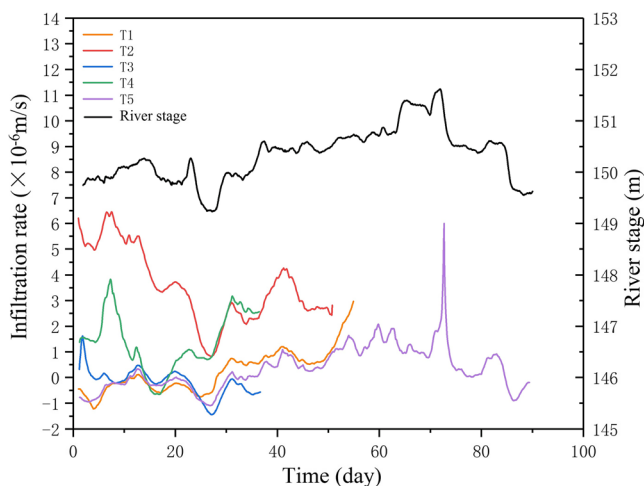

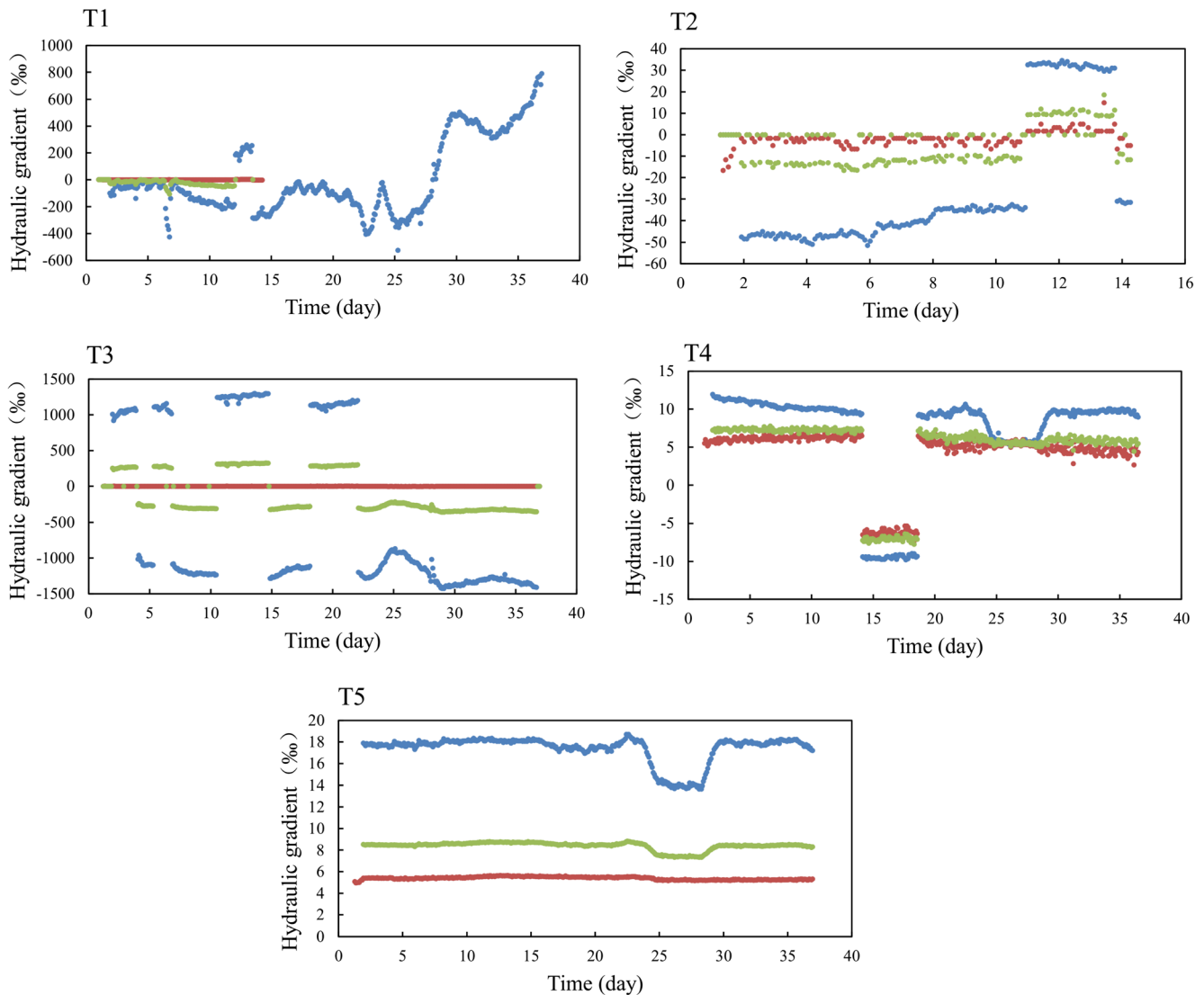Fig. 11 Variation in bank infiltration rate and river stage

Fig. 12 Variations of hydraulic gradient at each monitoring point (blue, red and green dots represent the hydraulic gradient of sediments in the ranges of 0–20, 20–80, and 0–80 cm below the bed surface, respectively)

shows that the results of the heat tracing are close to those of the standpipe experiment. Both methods employ in-situ monitoring and testing in the riverbed, so the data are reliable. However, the results from the empirical formula method are higher than from other methods due to the disturbance of the sediment particles during sample collection. Nevertheless, the variation trend of the empirical formula method is consistent with the other two methods.

Time-varying characteristics

Figure 11 shows that the hydraulic conductivity (K) of sediments of each layer at each monitoring point has the same trend, and the K value of bed sediments in the surface layer (0–20 cm) is smaller than that in the deep layer (20–80 cm). The results are discussed here for each monitoring point:

The edge of the sandbank (T1) The K value of each layer fluctuates violently. The K value of surface sediment (0–20 cm) fluctuates from 8.5×10^{-3} to 10.3 m/day, while that of the deep sediment (20–80 cm) fluctuates from 9.3×10^{-2} to 1.7×10^2 m/day. The difference between the surface layer and deep layer reaches two orders of magnitude at the same instant. The K value of surface sediments shows an obvious upward trend after each flood peak, while it shows a downward trend after the flood retreat.

The junction to the main channel and the sandbank (T2) The fluctuation of the K value of each layer is relatively flat in the 1st–10th day with an average value of 1.0 m/day in the surface layer (0–20 cm) and 18.0 m/day in the deep layer (20–80 cm). The river stage rises gradually after the 10th day and the fluctuation of the K value of sediments becomes more pronounced.

Fig. 13 Variations of sediment hydraulic conductivity at each monitoring point (K_1, K_2, and K_3 represent the hydraulic conductivity of sediments in the ranges of 0–20, 20–80, and 0–80 cm below the bed surface, respectively)
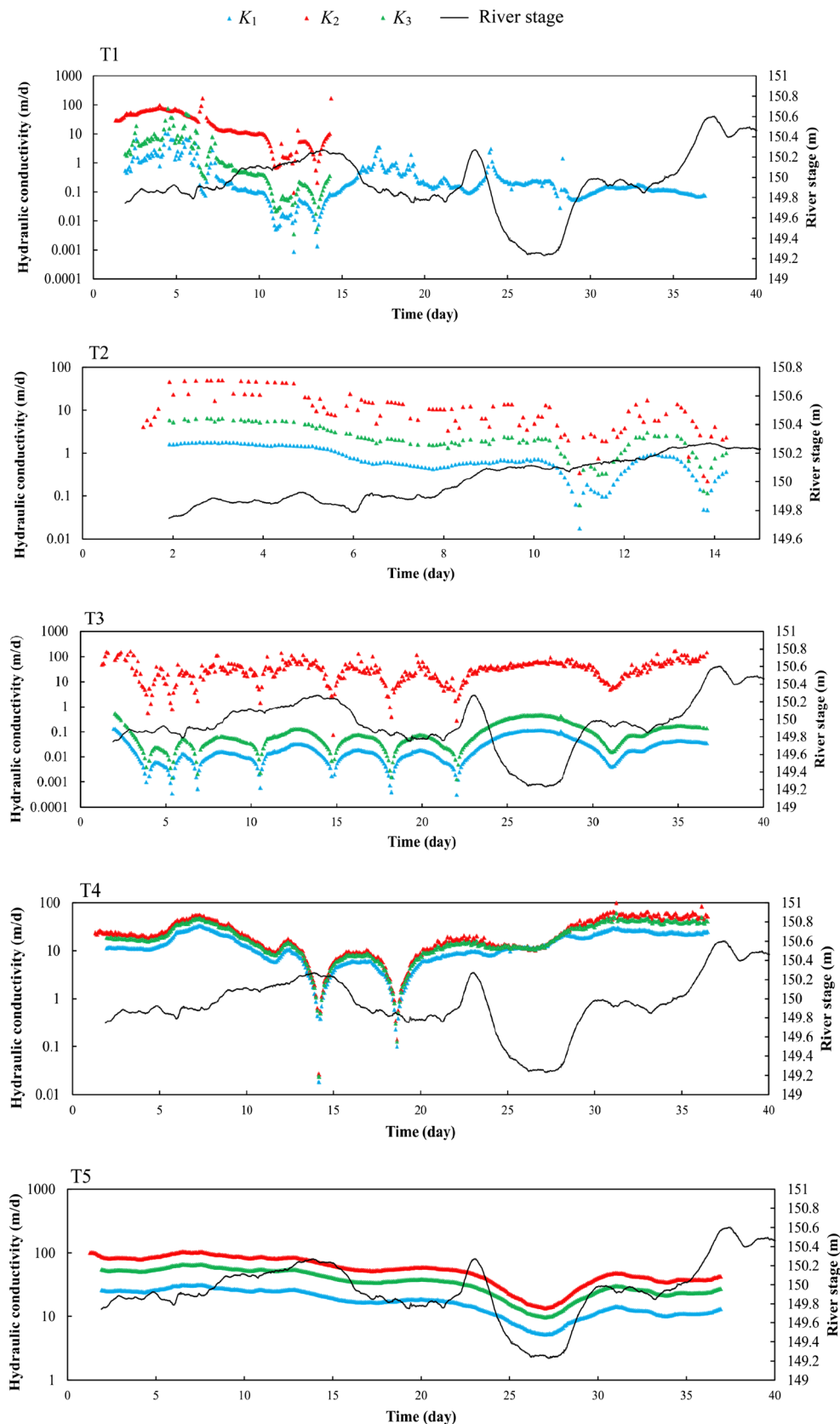
Table 1 Fluctuation range of sediment hydraulic conductivity at each monitoring point

Point number	Hydraulic conductivity, K (m/day)		
	Depth 0–20 cm	Depth 20–80 cm	Depth 0–80 cm
T1	8.5×10^{-4}–10.3	9.3×10^{-2}–168.2	3.5×10^{-3}–74.0
T2	5.2–31.4	13.4–104.5	9.6–65.8
T3	3.1×10^{-4}–1.3×10^{-1}	7.3×10^{-2}–167.9	1.3×10^{-3}–5.2×10^{-1}
T4	1.8×10^{-2}–32.6	2.6×10^{-2}–96.8	2.4×10^{-2}–59.6
T5	1.8×10^{-2}–7.78	2.2×10^{-1}–49.3	6.1×10^{-2}–6.4

Upstream of the channel bar (T3) The K value of each layer shows obvious periodic fluctuations. The K values of the surface layer (0–20 cm) and the deep layer (20–80 cm) fluctuate periodically from 3.1×10^{-4} to 1.3×10^{-1} m/day and from 7.3×10^{-2} to 1.7×10^{2} m/day, respectively. The values of the surface layer and deep layer differ greatly with a maximum difference of four orders of magnitude at the same time. The fluctuations lag behind the variation in the river stage to some extent during the flood process.

Downstream of the channel bar (T4) The K values of each layer are close to each other and show no obvious correlation with the change of river stage during the flood process. The lowest K value occurs on days 14 and 19, which are 1.8×10^{-2} m/day and 2.3×10^{-1} m/day in the surface layer (0–20 cm), and 2.6×10^{-2} m/day and 1.4×10^{-1} m/day in the deep layers (20–80 cm), respectively.

The main channel (T5) The fluctuation of the K value of each layer is relatively flat. On the 25th day, the K value of sediments decreases significantly from 16.4 to 6.0 m/day in the surface layer (0–20 cm) and from 49.3 to 13.4 m/day in the deep layer (20–80 cm) in an obvious flood retreat process, and rises again when the flood returns.

The preceding results indicate that the hydraulic conductivity of riverbed sediments has a strong spatio-temporal variation, and has some correlation with the river stage fluctuation during different parts of the flood process, but it does not completely depend on the river stage
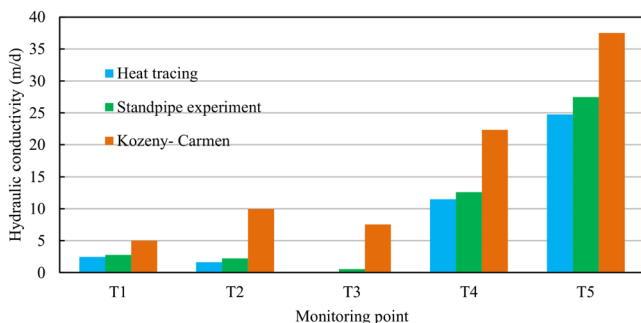
Fig. 14 Comparison of calculation results of sediment hydraulic conductivity

changes. It is helpful to quantify and predict the hydraulic conductivity of riverbed sediments by understanding the characteristics of the hydrodynamic conditions and the riverbed morphology.

Discussion

Comparison of methods

The riverbed is a key factor controlling river–groundwater interaction, and the composition of the riverbed is continuously affected by sedimentation and erosion (Coleman 1969; Levy et al. 2011) and chemical and biological processes (Du et al. 2013; Smith and Lerner 2008). At present, there are many methods for evaluating the transience of riverbed sediment properties—for example, traditional methods include the use of seepage meters (Rosenberry 2008; Woessner and Sullivan 1984), permeameters (Landon et al. 2001; Lee et al. 2015), laboratory measurements of streambed samples (Rosenberry and Pitlick 2009; Schälchli 1992), and thermal methods (Hatch et al. 2010; Mutiti and Levy 2010). Some emerging methods such as a floodwave response model, which only needs data of time series of stream stage and near-stream hydraulic head as input (Gianni et al. 2016), and the fully integrated hydrological model HydroGeoSphere, were also applied for the same objective (Tang et al. 2018). Opportunities for new research within the coupled framework of different disciplines such as sedimentology, hydrology, and hydrogeology have also been discussed (Partington et al. 2017). Although the integration of various approaches and disciplines is advancing, major research gaps remain to be filled to allow more complete and quantitative integration across disciplines (Brunner et al. 2017). The thermal method is a new and reliable method that has been employed in recent years. Although it can calculate the exchange flux between surface water and groundwater within the riverbed, it cannot obtain the hydraulic conductivity of the sediment without continuous monitoring of hydraulic gradients. Therefore, this study used heat as a tracer, combined with measured river stage and pore-water heads at different depths in the sediment, to calculate the variation of the hydraulic conductivity of the riverbed sediment. To the authors' knowledge,

representation of time-series data of riverbed sediment hydraulic conductivity by point monitoring during the riverbed sediment flushing and clogging has not been reported in other related studies.

Uncertainty and limitations

It is assumed that the shallow layer of the riverbed is dominated by vertical flow. This report does not discuss the anisotropy of the sediment hydraulic conductivity, but only focuses on the vertical. Nevertheless, the simplification of the riverbed properties will result in deviation of the calculation or simulation of the interaction between surface water and groundwater in the RBF system. Anisotropy has also been strongly suggested as an additional calibration parameter when performing hydrogeological simulations (Gianni et al. 2019).

This study considered the vertical heterogeneity of the sediment by calculating the hydraulic conductivity at different depths, on which scale the results can achieve a certain accuracy according to comparison of the results of the standpipe experiment and empirical relations (Kozeny-Carmen). However, the apparent horizontal heterogeneity of the riverbed sediment caused by the flushing and clogging process is difficult to evaluate based on the point monitoring method. This may require simulation and prediction through numerical models (Tang et al. 2018)—for example, by simulating and predicting the transience of the particle-size distribution of riverbed sediment and quantifying the relationship between particle size and hydraulic conductivity, it is possible to simulate and predict the horizontal heterogeneity of the riverbed.

Characteristics of the aquifer adjacent to the river also strongly influence the interaction between surface water and groundwater. When the hydraulic conductivity of riverbed sediments is lower than that of the aquifer, an unsaturated zone can develop under the riverbed, resulting in the weakening or disappearance of the connection between surface water and groundwater (Fox and Durnford 2003; Su et al. 2007; Lamontagne et al. 2014). As part of this work, sediment samples were collected from 18 points of the riverbed within the study area in different seasons. It was found that the sediment of the Second Songhua River bed is generally dominated by sand, and lenses with very low permeability appear very infrequently on or below the sediment surface. In this case, due to the effect of lateral flow, the river bed may still remain saturated (Schilling et al. 2017). In addition, the amount of groundwater extraction is only 5,900 m³/day and previous measurements of groundwater level on the river bank showed that river water and groundwater are continuously connected. Therefore, in this study, it was assumed that the medium under the riverbed is saturated.

The variation of hydraulic gradient (Fig. 12) indicates that there is a phenomenon of alternating recharge of surface water and groundwater. Research shows that upward infiltrating groundwater may cause an unclogging of the riverbed (Gianni et al. 2016), but this is minimal compared to the impact of river-water flushing, because the erosion caused by river-water flushing may wash away a certain thickness of sediments, while the infiltration of groundwater can at most only drive fine particles away from the sediment pores.

Conclusions

The infiltration rate of river water in riverbed sediments fluctuates and there is a significant positive correlation between the infiltration rate and the river stage. The temporal and spatial variation in the riverbed sediment hydraulic conductivity is not entirely related to the river stage fluctuation, but also subject to hydrodynamic conditions, riverbed topography, riverbed sediment lithology, and other factors during the process of sediment flushing and clogging. The hydraulic conductivity of the sediment in the main channel is significantly higher than that of the channel bar, sandbank, and riverbank. When affected by the clogging process under weak hydrodynamic conditions, the sediment hydraulic conductivity is relatively low, especially at the riverbank where the presence of a relatively thick silt layer makes the sediment almost impermeable.

Heat tracing and water-level monitoring can obtain data on the dynamic changes in hydraulic conductivity of the riverbed sediment. Sediment particle-size analysis, combined with point measurements, innovatively revealed the response of bank infiltration rate and riverbed properties to changes in river hydrological conditions. However, the method may not be applicable to riverbeds with larger or smaller particles such as pumice stones in the upstream of rivers and silt in the downstream of rivers, because it may cause the piezometer and temperature sensors to be damaged and the filter screen to be blocked during the downward drilling. Nevertheless, for sandy riverbeds, this method still has great application value. When the standpipe experimental approach and the empirical formula calculation are used, the measuring points of each campaign need to be consistent and the measuring frequency should be increased. Understanding the variation in bank infiltration rate and sediment hydraulic conductivity during sediment flushing and clogging is the basis for the evaluation of groundwater resources in this RBF site and provides a scientific framework for calculating river recharge to groundwater during flooding. This work can inform future RBF projects along the Second Songhua River where water resource management may be critical for both domestic and industrial use.

References

Ahmed AKA, Marhaba TF (2016) Review on river bank filtration as an in situ water treatment process. Clean Techn Environ Policy 19(2):1–11

Anibas C, Buis K, Verhoeven R, Meire P, Batelaan O (2011) A simple thermal mapping method for seasonal spatial patterns of groundwater–surface water interaction. J Hydrol 397(1–2):93–104

Battin TJ, Sengschmitt D (1999) Linking sediment biofilms, hydrodynamics, and river bed clogging: evidence from a large river. Microb Ecol 37(3):185–196

Baveye P, Vandevivere P, Hoyle BL, Deleo PC, Lozada DS (1998) Environmental impact and mechanisms of the biological clogging of saturated soils and aquifer materials. Crit Rev Environ Sci Technol 28(2):123–191

Blaschke AP, Steiner KH, Schmalfuss R, Gutknecht D, Sengschmitt D (2010) Clogging processes in Hyporheic interstices of an impounded river, the Danube at Vienna, Austria. Int Rev Hydrobiol 88(3–4):397–413

Bourg ACM, Bertin C (1993) Biogeochemical processes during the infiltration of river water into an alluvial aquifer. Environ Sci Technol 27(4):661–666

Brunner P, Therrien R, Renard P, Simmons CT, Franssen HJH (2017) Advances in understanding river–groundwater interactions. Rev Geophys 55(3):818–854

Carrier WD (2003) Goodbye, Hazen; hello, Kozeny-Carman. J Geotech Geoenviron 129(11):1054–1056

Cey EE, Rudolph DL, Parkin GW, Aravena R (1998) Quantifying groundwater discharge to a small perennial stream in southern Ontario, Canada. J Hydrol 210(1–4):21–37

Chen X (2004) Streambed hydraulic conductivity for rivers in south-central Nebraska. JAWRA J Am Water Resour Assoc 40(3):13

Coleman JM (1969) Brahmaputra river: channel processes and sedimentation. Sediment Geol 3(2–3):129–239

Crosbie RS, Taylor AR, Davis AC, Lamontagne S, Munday T (2014) Evaluation of infiltration from losing-disconnected rivers using a geophysical characterisation of the riverbed and a simplified infiltration model. J Hydrol 508:102–113

Danczak RE, Sawyer AH, Williams KH, Stegen JC, Hobson C, Wilkins MJ (2016) Seasonal hyporheic dynamics control coupled microbiology and geochemistry in Colorado River sediments. J Geophys Res: Biogeosci 121:2976–2987. https://doi.org/10.1002/2016JG003527

Datry T, Lamouroux N, Thivin G, Descloux S, Baudoin JM (2015) Estimation of sediment hydraulic conductivity in river reaches and its potential use to evaluate streambed clogging. River Res Appl 31(7):880–891

Domenico PAF, Schwartz F (1997) Physical and chemical hydrogeoloy, 2nd edn. Wiley, chichester, UK

Du X, Wang Z, Ye X (2013) Potential clogging and dissolution effects during artificial recharge of groundwater using potable water. Water Resour Manag 27(10):3573–3583

Engesgaard P, Seifert D, Herrera P (2006) Bioclogging in porous media: tracer studies. Riverbank Filtr Hydrol 60:93–118

Farnsworth CE, Hering JG (2011) Inorganic geochemistry and redox dynamics in bank filtration settings. Environ Sci Technol 45(12):5079–5087

Febria CM, Fulthorpe RR, Williams DD (2010) Characterizing seasonal changes in physicochemistry and bacterial community composition in hyporheic sediments. Hydrobiologia 647(1):113–126

Fischer T, Day K, Grischek T (2005) Sustainability of riverbank filtration in Dresden, Germany. In: Recharge systems for protecting and enhancing groundwater resources. UNESCO IHP-VI Series on Groundwater 13, Proc. Int. Symp. Management of Artificial Recharge, Berlin, June 2005, pp 23–28

Fox GA, Durnford DS (2003) Unsaturated hyporheic zone flow in stream/aquifer conjunctive systems. Adv Water Resour 26(9):989–1000

Frei S, Fleckenstein JH, Kollet SJ, Maxwell RM (2009) Patterns and dynamics of river–aquifer exchange with variably-saturated flow using a fully-coupled model. J Hydrol 375(3–4):383–393

Gianni G, Richon J, Perrochet P, Vogel A, Brunner P (2016) Rapid identification of transience in streambed conductance by inversion of floodwave responses. Water Resour Res 52(4):2647–2658

Gianni G, Doherty J, Brunner P (2019) Conceptualization and calibration of anisotropic alluvial systems: pitfalls and biases. Groundwater 57(3):409–419

Goldschneider AA, Haralampides KA, Macquarrie KTB (2007) River sediment and flow characteristics near a bank filtration water supply: implications for riverbed clogging. J Hydrol 344(1):55–69

Gordon RP, Lautz LK, Briggs MA, McKenzie JM (2012) Automated calculation of vertical pore-water flux from field temperature time series using the VFLUX method and computer program. J Hydrol 420(4):142–158

Gorman PD, Constantz J, Laforce MJ (2007) Spatial and temporal variability of hydraulic properties in the Russian River streambed, central Sonoma County, California. AGU Fall Meeting, Abstracts, San Francisco, December 2007

Grischek T, Bartak R (2016) Riverbed clogging and sustainability of riverbank filtration. Water 8(12):604

Gurnell AM, Bertoldi W, Corenblit D (2012) Changing river channels: the roles of hydrological processes, plants and pioneer fluvial landforms in humid temperate, mixed load, gravel bed rivers. Earth Sci Rev 111(1–2):129–141

Hatch CE, Fisher AT, Ruehl CR, Stemler G (2010) Spatial and temporal variations in streambed hydraulic conductivity quantified with time-series thermal methods. J Hydrol 389(3–4):276–288

Hart DR, Mulholland PJ, Marzolf ER, Deangelis D, Hendricks S (1999) Relationships between hydraulic parameters in a small stream under varying flow and seasonal conditions. Hydrol Process 13(10):1497–1510

Harvey J, Gooseff M (2015) River corridor science: hydrologic exchange and ecological consequences from bedforms to basins. Water Resour Res 51(9):6893–6922

Hvorslev MJ (1951) Time lag and soil permeability in ground-water observations. US Army Bull 36(118):1–50

Jolly ID, Mcewan KL, Holland KL (2008) A review of groundwater–surface water interactions in arid/semi-arid wetlands and the consequences of salinity for wetland ecology. Ecohydrology 1(1):43–58

Schubert J (2003) German experience with riverbank filtration systems. Riverbank Filtr Hydrol 43:35–48

Kozeny J (1927) Uber kapillare leitung der wasser in Boden [On the conductivity of water in the soil]. J Geosci Environ Protect 136A:271–306

Lamontagne S, Taylor AR, Cook PG, Crosbie RS, Brownbill R, Williams RM, Brunner P (2014) Field assessment of surface water–groundwater connectivity in a semi-arid river basin (Murray–Darling, Australia). Hydrol Process 28(4):1561–1572

Landon MK, Rus DL, Harvey FE (2001) Comparison of instream methods for measuring hydraulic conductivity in sandy streambeds. Groundwater 39(6):870–885

Lee BJ, Lee JH, Yoon H, Lee E (2015) Hydraulic experiments for determination of in-situ hydraulic conductivity of submerged sediments. Sci Rep 5:7917

Lee DR (1979) A field exercise on groundwater flow using seepage meters and mini-piezometers. J Geol Educ 27:6–10

Leonardson R (2011) Exchange of fine sediments with gravel riverbeds. PhD Thesis, Univ. of California, Berkeley, CA

Levy J, Birck MD, Mutiti S, Kilroy KC, Windeler B, Idris O, Allen LN (2011) The impact of storm events on a riverbed system and its hydraulic conductivity at a site of induced infiltration. J Environ Manag 92(8):1960–1971

Liao Z, Lin X, Shi Q, Yang S, Du X (2004) Experimental study on groundwater exploitation in Weihe River in the lower Yellow River: a case study of the Yellow River Beach in the northern suburbs of Zhengzhou (in Chinese). Scient Sin Technol 34(S1):13–22

Mueller ER, Pitlick J (2013) Sediment supply and channel morphology in mountain river systems: 1. relative importance of lithology, topography, and climate. J Geophys Res: Earth Surf 118(4):2325–2342

Mutiti S, Levy J (2010) Using temperature modeling to investigate the temporal variability of riverbed hydraulic conductivity during storm events. J Hydrol 388(3–4):321–334

Nogaro G, Datry T, Mermillod-Blondin F, Descloux S, Montuelle B (2010) Influence of streambed sediment clogging on microbial processes in the hyporheic zone. Freshw Biol 55(6):1288–1302

Nosrati K (2017) Ascribing soil erosion of hillslope components to river sediment yield. J Environ Manag 194:63–72

Odong J (2007) Evaluation of empirical formulae for determination of hydraulic conductivity based on grain-size analysis. J Am Sci 3(3):54–60

Partington D, Therrien R, Simmons CT, Brunner P (2017) Blueprint for a coupled model of sedimentology, hydrology, and hydrogeology in streambeds. Rev Geophys 55(2):287–309

Pholkern K, Srisuk K, Grischek T, Soares M, Schäfer S, Archwichai L, Saraphirom P, Pavelic P, Wirojanagud W (2015) Riverbed clogging experiments at potential river bank filtration sites along the Ping River, Chiang Mai, Thailand. Environ Earth Sci 73(12):7699–7709

Ray C, Melin G, Linsky RB (2002) Riverbank filtration: improving source water quality. Bull Am Meteorol Soc 84(10):1428

Rosenberry DO (2000) Unsaturated-zone wedge beneath a large, natural lake. Water Resour Res 36(12):3401–3409

Rosenberry DO (2008) A seepage meter designed for use in flowing water. J Hydrol 359(1–2):118–130

Rosenberry DO, Pitlick J (2009) Effects of sediment transport and seepage direction on hydraulic properties at the sediment–water interface of hyporheic settings. J Hydrol 373(3–4):377–391

Schälchli U (1992) The clogging of coarse gravel river beds by fine sediment. Hydrobiologia 235:189–197

Schilling OS, Irvine DJ, Franssen HH, Brunner P (2017) Estimating the spatial extent of unsaturated zones in heterogeneous river–aquifer systems. Water Resour Res 53(12):10583–10602

Seifert D, Engesgaard P (2007) Use of tracer tests to investigate changes in flow and transport properties due to bioclogging of porous media. J Contam Hydrol 93(1–4):58–71

Simpson SC, Meixner T (2010) Temporal variations in riverbed hydraulic properties due to sediment transport during floods: implications for groundwater–surface water interaction and composition. AGU Fall Meeting, Abstracts, San Fransisco, September 2010

Smith JWN, Lerner DN (2008) Geomorphologic control on pollutant retardation at the groundwater–surface water interface. Hydrol Process 22(24):4679–4694

Springer AE, Petroutson WD, Semmens BA (1999) Spatial and temporal variability of hydraulic conductivity in active reattachment bars of the Colorado River, Grand Canyon. Groundwater 37(3):338–344

Stallman RW (1965) Steady one-dimensional fluid flow in a semi-infinite porous medium with sinusoidal surface temperature. J Geophys Res 70(12):2821–2827

Stéphanie RP, Ragusa S, Sztajnbok P, Vandevelde T (2000) Interrelationships between biological, chemical, and physical processes as an analog to clogging in aquifer storage and recovery (ASR) wells. Water Res 34(7):2110–2118

Stewardson MJ, Datry T, Lamouroux N, Pella H, Thommeret N, Valette L, Grant SB (2016) Variation in reach-scale hydraulic conductivity of streambeds. Geomorphology 259:70–80

Su GW, Constantz J, Jasperse J, Seymour D (2002) Use of ground-water temperature patterns to determine the hydraulic conductance of the streambed along the middle reaches of the Russian River, CA. AGU Fall Meeting Abstracts, San Francisco, September 2002

Su GW, Jasperse J, Seymour D, Constants J (2004) Estimation of hydraulic conductivity in an alluvial system using temperatures. Ground Water 42(6–7):890–901

Su GW, Jasperse J, Seymour D, Constantz J, Zhou Q (2007) Analysis of pumping-induced unsaturated regions beneath a perennial river. Water Resour Res 43:W08421. https://doi.org/10.1029/2006WR005389

Su X, Cui G, Du S, Yuan W, Wang H (2016) Using multiple environmental methods to estimate groundwater discharge into an arid lake (Dakebo Lake, Inner Mongolia, China). Hydrogeol J 24(7):1–16

Su X, Lu S, Gao R, Su D, Yuan W, Dai Z, Papavasilopoulos EN (2017a) Groundwater flow path determination during riverbank filtration affected by groundwater exploitation: a case study of Liao River, Northeast China. Hydrol Sci J/J Des Sci Hydrol 62(14):2331–2347. https://doi.org/10.1080/02626667.2017.1383609

Su X, Cui G, Wang H, Dai Z, Woo NC, Yuan W (2017b) Biogeochemical zonation of sulfur during the discharge of groundwater to lake in desert plateau (Dakebo Lake, NW China). Environ Geochem Health 40(3):1051–1066

Su X, Lu S, Yuan W, Woo NC, Dai Z, Dong W, Du S, Zhang X (2018) Redox zonation for different groundwater flow paths during bank filtration: a case study at Liao River, Shenyang, northeastern China. Hydrogeol J 26(5):1573–1589

Tang Q, Schilling OS, Kurtz W, Brunner P, Vereecken H, Franssen HJH (2018) Simulating flood-induced riverbed transience using unmanned aerial vehicles, physically based hydrological modeling, and the ensemble Kalman filter. Water Resour Res 54(11):9342–9363

Ulrich C, Hubbard SS, Florsheim JL, Rosenberry D, Borglin SE, Trotta M, Seymour D (2015) Riverbed clogging associated with a California riverbank filtration system: an assessment of mechanisms and monitoring approaches. J Hydrol 529:1740–1753

Wang L, Meng X, Xu H (2006) Analysis of causes of excessive Fe and Mn content in source water of catchment areas in Jiamusi City (in Chinese). Environ Sci Manag 31(1):152–153

Woessner WW, Sullivan KE (1984) Results of seepage meter and mini-piezometer study, Lake Mead, Nevada. Ground Water 22(5):561–568

Zhang Y, Hubbard S, Finsterle S (2011) Factors governing sustainable groundwater pumping near a river. Groundwater 49(3):432–444